Original Paper

phys. stat. sol. (a) **202**, No. 1, 102–107 (2005) / **DOI** 10.1002/pssa.200406906

Cathodoluminescent characteristics of Sm-doped $ZnAl_2O_4$ nanostructured powders

E. Martinez-Sanchez[1], **M. Garcia-Hipolito**[1], **J. Guzman**[1], **F. Ramos-Brito**[1], **J. Santoyo-Salazar**[1], **R. Martinez-Martinez**[1], **O. Alvarez-Fregoso**[*, 1], **M. I. Ramos-Cortes**[2], **J. J. Mendez-Delgado**[2], and **C. Falcony**[2]

[1] Instituto de Investigaciones en Materiales-UNAM, Apdo. Postal 70-360, México D.F., Coyoacán 04510, México

[2] Departamento de Física, CINVESTAV-IPN, Apdo. Postal 14-740, 07000, México D.F., México

Received 24 June 2004, revised 14 September 2004, accepted 22 October 2004
Published online 10 December 2004

PACS 78.60.Hk, 78.67.Bf, 81.07.Bc, 81.20.Ka

Cathodoluminescent (CL) powders of zinc aluminate activated with samarium ions have been prepared by a co-precipitation chemical process. Different doping concentrations in the start mixture and sintering temperatures for the precipitated powder were studied. It was observed that the crystalline characteristics of the powders depend upon the sintering temperature. For temperatures higher than 450 °C, the powders presented the cubic spinel phase with a lattice parameter value of 8.0756 Å, and grain sizes from 50 to 100 nm with semispherical shape. The CL emission spectra showed broad bands localized at 564, 602, 644, and 703 nm associated with $^4G_{5/2} \rightarrow {}^6H_{5/2}$, $^4G_{5/2} \rightarrow {}^6H_{7/2}$, $^4G_{5/2} \rightarrow {}^6H_{9/2,}$ and $^4G_{5/2} \rightarrow {}^6H_{11/2}$ transitions in the Sm^{3+} ions, respectively. Concentration quenching of the cathodoluminescence occurred at about 4.26 at% of the activator (Sm) concentration inside the sintered powders.

1 Introduction

Zinc aluminate ($ZnAl_2O_4$) is a well-known wide bandgap semiconductor with a spinel structure [1, 2] and an optical bandgap of 3.8 eV (i.e., transparent for light wavelengths greater than 320 nm). Thus, it can be used in ultraviolet photoelectronics devices and when doped with rare-earth optical activators it can be used as luminescent material. Cathodoluminescent (CL) materials are widely used in modern cathode-ray tube (CRT)-based displays. $ZnAl_2O_4$ spinel has also been used in many catalytic reactions, such as cracking, dehydration of saturated alcohols to olefins [3], preparation of polymethylbenzenes, methanol and higher alcohol synthesis [4], and also as a support for alkane dehydrogenation catalysis [5, 6].

The preparation of nanocrystalline materials from solution-based chemical approaches is expected to achieve: (a) chemically homogeneous and phase-pure specimens, (b) low crystallization and sintering temperatures of the materials, and (c) narrow-sized distribution of particles. Various mixed oxides with a single phase and controlled particle size and morphology can be synthesized by co-precipitation chemical techniques and reaction sintering [7–10]. This paper reports the CL characteristics of samarium-doped $ZnAl_2O_4$ nanostructured powders, prepared by a co-precipitation chemical technique and sintered at low temperatures. The behavior of the CL spectra was studied as a function of the sintering temperature, the activator concentration, and the electron-accelerating potential. In addition, nanostructured grain sizes [11] and the crystalline structure of the powders as a function of the sintering temperatures were reported.

[*] Corresponding author: e-mail: oaf@servidor.unam.mx

2 Experimental process

The co-precipitation technique [12] was used for powder synthesis of zinc aluminate spinel powder doped with samarium. The start materials were: zinc acetate ($Zn(CH_3COO)_2 \cdot 2H_2O$, Aldrich Chemical Co.) and aluminum chloride hexahydrate ($AlCl_3 \cdot 6H_2O$, Aldrich Chemical Co.) at 0.05 M blended with ethanol. Doping with samarium was achieved by adding $SmCl_3 \cdot 6H_2O$ (Aldrich Chemical Co.) in the range 0–16 at% (a/o) in relation to the zinc content in the mixture. The initial mixture was heat treated at 260 °C with continuous stirring for 4 h to evaporate the solvent. The precipitated agglomerates were crushed in an agate mortar to obtain a fine powder. The powders were annealed in air at low temperatures (T_a) in a preheated laboratory quartz tube furnace coupled with a temperature controller (±0.5 °C) in the range 450–750 °C for 120 min, in increments of 100 °C.

The crystalline structure of the powders was analyzed by X-ray diffraction (XRD) using a Bruker AXS-D8 Plus Diffractometer with CuKα radiation at 1.5405 Å. Particle size and shape measurements were performed by atomic force microscopy (AFM), using a Jeol JSPM-421 in AC mode with silicon cantilever CSC15/25 Ultrasharp. Chemical composition was determined by energy dispersive spectroscopy (EDS) using an Oxford Pentafet with a beryllium window X-ray detector. Cathodoluminescent measurements were performed in a stainless steel vacuum chamber with a cold cathode electron gun (Luminoscope, model ELM-2; MCA, Relion Co.). Samples were placed inside the vacuum chamber and evacuated to 10^{-3} Torr. The electron gun was deflected at 90° to bombard the luminescent material perpendicular to the surface. The emitted light from the sample was coupled into an optical fiber bundle leading to a Perkin–Elmer LS50B fluorescence spectrophotometer. All CL spectra were obtained at room temperature. The accelerating voltage of the electron beam, used in the measurements reported, was in the range from 2 to 12 kV and the applied current was kept constant at 0.05 mA. The spot size of the electron beam on the sample surface was approximately 3 mm in diameter, which implies a current density of about 70 μA/cm^2.

3 Results and discussion

The crystallographic structure in the as-grown and annealed powders was established by the powder XRD technique (Fig. 1). The as-grown product was amorphous and formed by agglomerate powder.

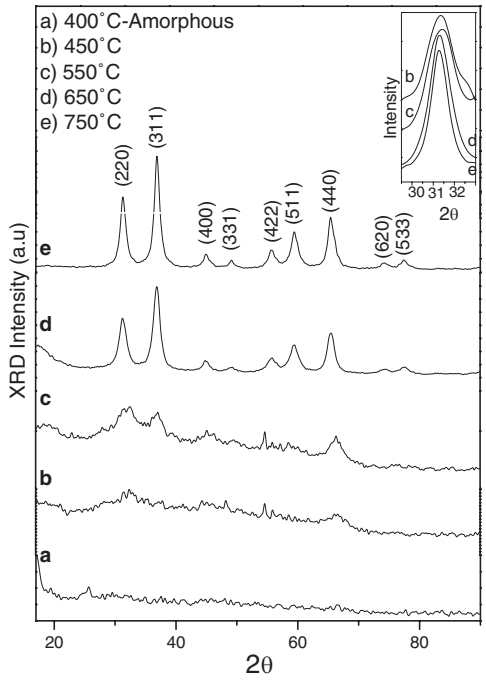

Fig. 1 XRD patterns for $ZnAl_2O_4:Sm^{3+}$ (2.23 at%) powders as a function of sintering temperature.

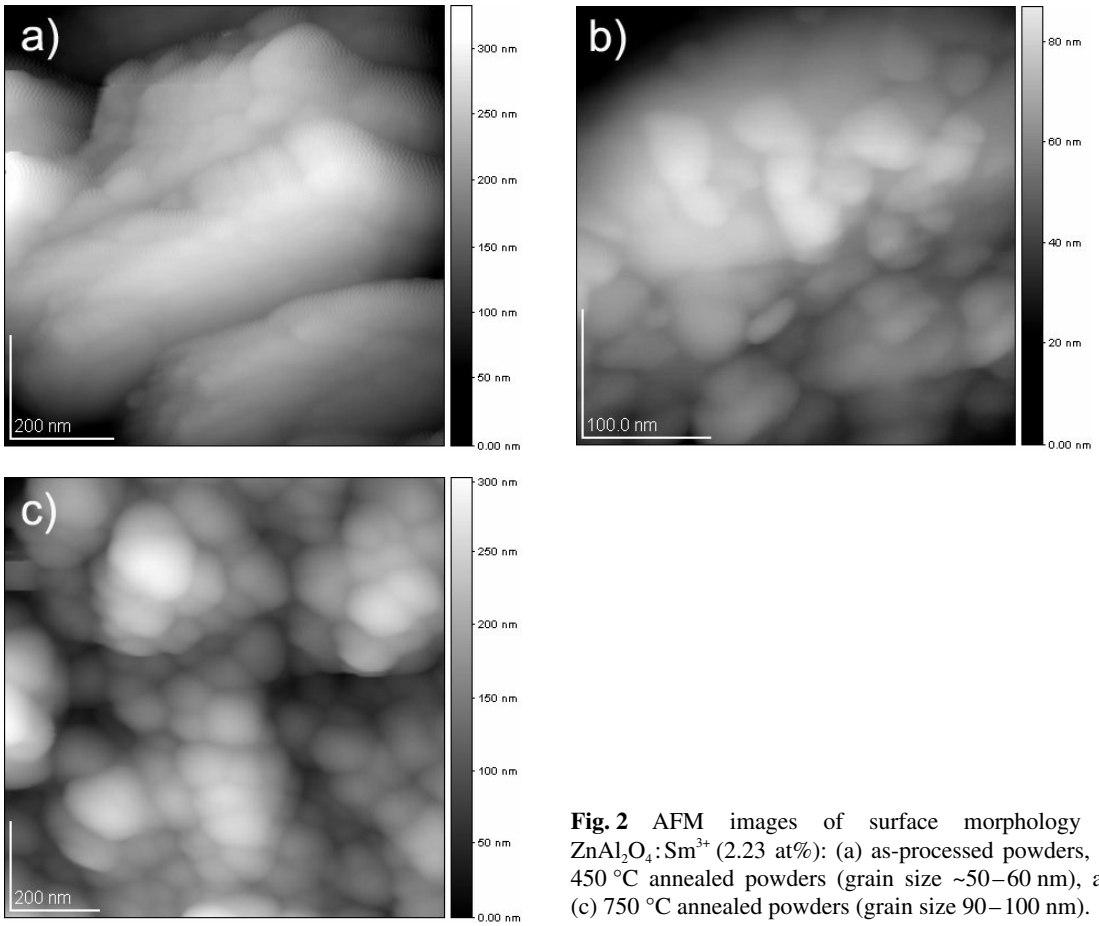

Fig. 2 AFM images of surface morphology of $ZnAl_2O_4:Sm^{3+}$ (2.23 at%): (a) as-processed powders, (b) 450 °C annealed powders (grain size ~50–60 nm), and (c) 750 °C annealed powders (grain size 90–100 nm).

Whereas the samples have been sintered at 450–750 °C is was shown that $ZnAl_2O_4$-gahnite is the only crystalline phase present (ICCD Card File No. 5-669) [13]. The diffraction peaks in the samples annealed at temperatures above 550 °C show sharper profiles due to the recrystallization-ordering process and grain growth. The calculated lattice parameter: a = 8.0756 Å, for cubic spinel phase in the sample annealed at 750 °C, is in good agreement with the reported value: a = 8.0848 Å [13]. The determination of the crystallite size from the line-shape analysis of the diffraction peaks shows a variation from about 20 nm to 50 nm for the annealed samples. The effect of the peak broadening, due to the nanometric crystallites, is evident when comparing the (220) diffraction peak of the samples sintered from 450 to 750 °C (inset in Fig. 1).

The particle shape of the sintered powders was analyzed by recording AFM images of the same samples. As-precipitated powders (without grinding) consisted of agglomerates of lengths from 600 to 800 nm and diameters from 200 to 400 nm, as shown in Fig. 2(a). While the sintered powders consisted of agglomerates of semispherical particles, comprised of tiny nanocrystallites, the AFM images show crystallites of nearly uniform size of about 50–60 nm (see Fig. 2(b)) for the powder annealed at 450 °C, which grew on further heat treatment (at 750 °C) up to 90–100 nm (see Fig. 2(c)).

The EDS measurements performed on powders sintered at 750 °C with samarium concentration in the precursor mixture of 2, 4, 6, 8, and 16 at% indicated that approximately 25% of this material remained in the sintered powder (0.33, 0.85, 1.53, 2.23, and 4.26 at%, respectively). The CL emission spectra of $ZnAl_2O_4:Sm$ powders, as a function of the doping concentration, are shown in Fig. 3. These spectra exhibit three dominant bands centered at 564 nm, 602 nm, and 644 nm and a weak emission in the region

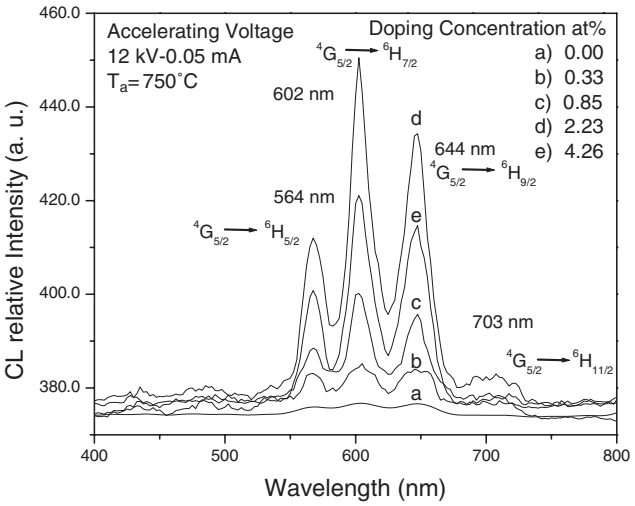

Fig. 3 Doping concentration dependence on the CL emission intensity of $ZnAl_2O_4:Sm^{3+}$ powders. T_a = 750 °C, V = 12 kV, I = 0.05 mA.

of 703 nm, which correspond to transitions between the $^4G_{5/2}$ and the $^6H_{5/2}$, $^6H_{7/2}$, $^6H_{9/2}$ and $^6H_{11/2}$ electronic energy levels of the Sm^{3+} ions, respectively [14]. The strongest emission occurs at 602 nm. In fact, as the Sm concentration increases the CL signal increases but at the concentration of 4.26 a quenching effect is observed. In the case of rare-earth optical activators, the optimal activator concentration occurs at different values for different types of excitation [15]. In order to CL, the impurities adsorbed at the surface of luminescent materials, as well as surface defects often become quenchers and may, by quenching the emission near the surface, produce a dead-voltage layer. However, migration of excitation by resonant energy transfer between rare-earth activators can be so efficient that it may carry the energy to a distant ion-killer existing at the surface of the luminescent material. Aggregation of doping activators at high concentrations may change some activators to quenchers and induce a related concentration quenching effect [16]. Other effects relative to quenching of CL are: thermal quenching due to local heating by energetic electrons of the CL electron beam on the luminescent surface material; by saturation of luminescent centers, where the majority of centers are already in an excited state, leaving an insufficient quantity of available centers in the ground state free to accept energy from the excited carriers [16, 17] and due to the Auger effect, which produce ejection of electrons leaving the luminescent center de-excited [18]. Furthermore, it is known that many cross-relaxation processes involving the $^4G_{5/2}$ to ^6F_j relaxation at the donor and $^6H_{5/2}$ to ^7F_J transitions at the acceptor (J = 5/2, 7/2, 9/2, and 11/2) can be involved in quenching the luminescence of Sm^{3+}-doped materials, as reported by Luxbacher et al. [19]. As the concentration of Sm increases from 0.33 to 4.26%, the Sm^{3+}–Sm^{3+} interactions are no longer negligible and quenching of the emission probably occurs due to cross-relaxation processes between neighboring Sm^{3+} ions, in a similar way as occurs in $Y_2O_3:Sm^{3+}$ nanocrystals, recently reported by Vetrone et al. [20]. As can be seen in Fig. 3, the maximum intensity emission is obtained for 2.23 at% of Sm ions incorporated into the sintered powders. Higher or lower Sm concentration resulted in less intense CL emissions.

It is commonly accepted that the magnetic dipole (md)-allowed transitions obey the selection rule $\Delta J = 0, \pm 1$. Then the transition $^4G_{5/2} \rightarrow {}^6H_{5/2}$ according to the first condition ($\Delta J = 0$), is an (md) in nature whose intensity remains without changing with the host matrix. The next transition $^4G_{5/2} \rightarrow {}^6H_{7/2}$ ($\Delta J = \pm 1$) is also an (md)-allowed one but, furthermore, it is electric dipole (ed) dominated. After this, it is partly an (md) and also partly an (ed) natured one. The transition $^4G_{5/2} \rightarrow {}^6H_{9/2}$ is purely an (ed) one which is sensitive to the crystal field [21, 22]. Usually, the intensity ratio of (ed) to (md) transitions is used to measure the symmetry of the local environment of the trivalent 4f ions. The greater the intensity of (ed) transition, the more the asymmetry nature [21]. In this study, $^4G_{5/2} \rightarrow {}^6H_{9/2}$ (ed) transition in the electronic levels of Sm ions is more intense than $^4G_{5/2} \rightarrow {}^6H_{5/2}$ (md) transition indicating the asymmetric nature of the zinc aluminate host.

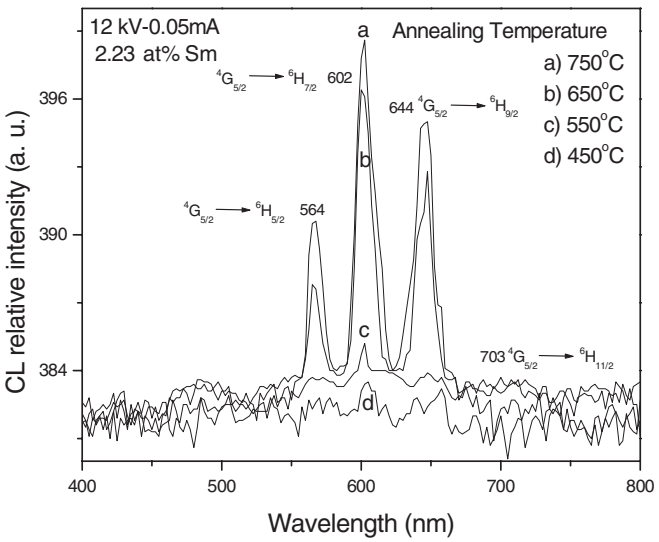

Fig. 4 Sintering temperature dependence on the cathodoluminescent emission intensity of $ZnAl_2O_4:Sm^{3+}$ (2.23 at%) powders. V = 12 kV, I = 0.05 mA.

Figure 4 shows the CL emission intensity behavior as a function of Ta for the 2.23 at% of Sm incorporated into the powders. The CL emission rises with increasing sintering temperature, suggesting that crystallite growth and reduction of structural defects in the powders favor radiative recombination mechanisms. Probably the reduction of chlorine and residual impurities left in the crystallized samples produce a better incorporation and distribution of Sm ions as an atomic impurity in the host lattice, which will result in an increase of the CL emissions as the sintering temperature is increased.

The dependence of the CL spectra measured under steady-state excitation on accelerating beam voltages in the range from 2 to 12 kV is shown in Fig. 5. The observed emission spectra shape remains unaffected by the accelerating voltage, which consists of four broad bands characteristic for the trivalent samarium ions. The overall emission intensity, however, is larger for higher electron-accelerating voltage showing no saturation effect in the voltage range studied. In principle, the incident electron beam reaches and penetrates the luminescent powders to generate secondary electrons and electron–hole pairs, which excite the activator ions in the host lattice and so generate CL emissions. As the electron accelerating voltage increases, the penetrating electrons produce more electron–hole pairs due to the interaction with a larger volume of the luminescent material and due to the higher generation rate of every incident elec-

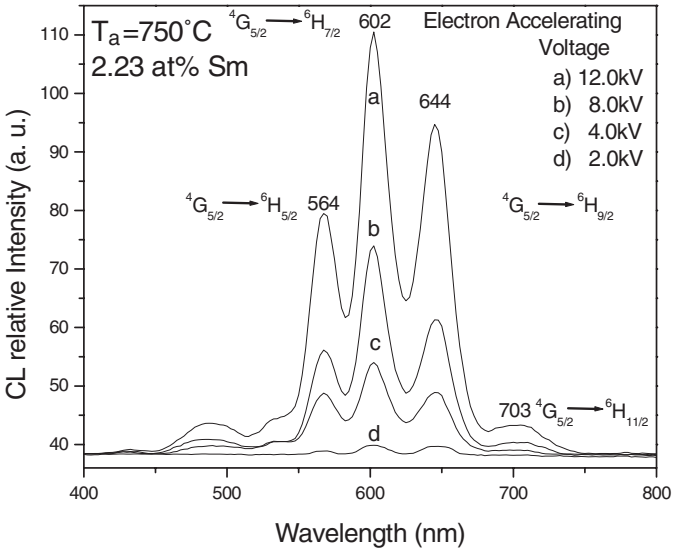

Fig. 5 Cathodoluminescent spectra of $ZnAl_2O_4:Sm^{3+}$ (2.23 at%) powders as a function of the electron accelerating voltage. T_a = 750 °C.

tron, resulting in much more intense activator luminescence because of the recombination of the electron–hole pairs. In addition, CL generation is complex due to the cascade nature of de-excitation, e.g., generated X-rays can provide a secondary means of CL production, known as roentgenoluminescence. Also, the production of secondary electrons is important to the CL-generation process, and they are generated along the entire zigzag path of energy dissipation, which may be many microns in length [23].

Finally, to the best of our knowledge, there are no reported studies on the synthesis, characterization, and luminescent properties of samarium-doped zinc aluminate nanostructured powders.

4 Conclusions

The cathodoluminescence and structural properties of nanostructured $ZnAl_2O_4:Sm^{3+}$ powders, synthesized using a co-precipitation low cost process, have been studied. The evolution of the crystalline structure and cathodoluminescent emission of these powders are strongly dependent on the sintering temperature. The powder particles were semi-spherical in shape with a grain size range of 50–60 nm for the powders annealed at 450 °C and of 90–100 nm for higher temperatures (750 °C). The crystallinity of the powders evolves into a well-defined cubic spinel structure phase with the lattice parameter a = 8.0756 Å as T_a is increased.

The cathodoluminescent spectra exhibited emission peaks associated with the electronic level transition of the Sm^{3+} ions, and its intensity rises as the sintered temperature increases. The optimal emission intensity was obtained with 8 at% of Sm^{3+} concentration doping in the initial mixture (2.23 at% inside the powders as measured by EDS). A concentration quenching was observed at high doping values. The red emission is the strongest and corresponds to the transition ($^4G_{5/2} \rightarrow {}^6H_{7/2}$) localized at 602 nm.

Acknowledgments The authors would like to thank Leticia Baños for the X-ray diffraction measurements and R. Reyes-Ortiz, J. García-Coronel, M. Guerrero, and Sarita Jimenez for their technical support.

References

[1] K. E. Sickfaus and J. M. Wills, J. Am. Ceram. Soc. **82**, 3279 (1998).
[2] S. Mathur, M. Veith, M. Haas, H. Shen, N. Lecerf, and V. Huch, J. Am. Ceram. Soc. **84**, 1921 (2001).
[3] T. K. Shioyama, Alcohol dehydratation employing a zinc aluminate catalysis, U.S. Patent 4,260,845 (1981).
[4] R. Szymanski, Ch. Travers, P. Chaumette, Ph. Courty, and D. Durand, Studies in Surface Science, Vol. 31 (Elsevier, Amsterdam, 1987), p. 739.
[5] M. A. Valenzuela, P. Bosch, G. Aguilar-Rios, B. Zapata, C. Maldonado, and I. Schifter, J. Mol. Cat. **84**, 177 (1993).
[6] G. Khare and R. A. Porter, Platinum and tin containing catalyst and use thereof in alkane dehydrogenation, U.S. Patent 5,430,220 (1995).
[7] G. Aguilar-Rios, M. Valenzuela, P. Salas, H. Armendariz, P. Bosch, G. Del Toro, R. Silva, V. Bertin, S. Castillo, A. Ramirez-Solis, and I. Schifter, Appl. Catal. A **127**(65) (1995).
[8] H. Wan-Shick and L. C. De Jonghe, J. Am. Ceram. Soc. **78**, 3217 (1995).
[9] C. Leblud, M. R. Anseau, E. Di Rupo, F. Cambier, and P. Fierens, J. Mater. Sci. Lett. **16**, 539 (1981).
[10] D. L. Branson, J. Am. Ceram. Soc. **48**, 591 (1965).
[11] H. Gleiter, Nanostruct. Mater. **6**, 3 (1995).
[12] E. Tani, M. Yoshimura, and S. Somiya, J. Am. Ceram. Soc. **64**, C181 (1981).
[13] Powder diffraction file card No. 5-669, International Center for Diffraction Data (1990).
[14] G. Blasse and B. C. Grabmaier, Luminescent Materials (Springer, Berlin, 1994).
[15] L. Osawa, H. Forest, P. M. Jaffe, and G. Ban, J. Electrochem. Soc. **118**, 482 (1971).
[16] T. Hase, T. Kano, E. Nakasawa, and H. Yamamoto, in: Phosphor materials for cathode-ray tubes, edited by P. W. Hawkes, Advanced in Electronics and Electron Physics, Vol. 79 (Academic Press, New York, 1990), p. 271.
[17] D. M. de Leeuw and G. W. T. Hoof, J. Lumin. **28**, 275 (1983).
[18] S. Imanaga, S. Yocono, and T. Hosima, Jpn. J. Appl. Phys. **19**, 41 (1980).
[19] T. Luxbacher, H. P. Fritzer, R. Sabry-Grant, and C. D. Flint, Chem. Phys. Lett. **241,** 103 (1995).
[20] F. Vetrone, J. Ch. Boyer, J. A. Capobianco, A. Speghini, and M. Bettinelli, Nanotechnology **15**, 75 (2004).
[21] K. Annapurna, R. N. Dwivedi, P. Kundu, and S. Buddhudu, Mater. Res. Bull. **38**, 429 (2003).
[22] P. S. May, D. H. Matcalf, F. S. Richardson, R. C. Carter, C. E. Miller, and R. A. Palmer, J. Lumin. **51**(5), 249 (1992).
[23] S. Myhajlenco, in: Luminescence of Solids, edited by D. R. Vij (Plenum Press, New York, 1998), chap. 4.